A multiscale approach to concrete fracture: the influence of the aggregate grading

Alberto Carpinteri, Pietro Cornetti
Department of Structural and Geotechnical Engineering
Politecnico di Torino, Torino, Italy

Abstract

The fractal approach to the mechanics of materials with disordered microstructure allows an elegant and unified explanation of the size effects the cohesive crack model parameters are subjected to. The aim of this work is to show why fractal patterns in the failure process of concrete specimens under tensile loads can be seen as a consequence of the grain size distribution of the aggregates. Finally, a fractal cohesive model will be outlined and applied to the most relevant test data.

1 Introduction

One of the most important topics in solid mechanics is the study of the so-called *size effect*, whose importance has been widely recognized during the last decades. With size effect we mean the dependence of one or more material parameters on the size of the structure made by that material. Particularly, in concrete-like materials tensile strength decreases with size, whereas fracture energy increases.

Such variations are mainly due to the localization of the damage in the failure process of the structures composed by quasi-brittle materials. Nowadays, the most used model to describe damage localization in materials with disordered microstructure (also called quasi-brittle or concrete-like materials) is the *cohesive crack model*, introduced by Hillerborg et al. [1]. According to Hillerborg's model, the material is characterized by a stress-strain relationship (σ-ε), valid for the undamaged zones, and by a stress-crack opening displacement relationship (σ- w, the cohesive law), describing how the stress decreases from its maximum value σ_u to zero as the distance between the crack lips increases from zero to the critical displacement w_c. The area below the cohesive law represents the energy $\mathcal{G}_F$ spent to create the unit crack surface. The cohesive crack model is able to simulate tests where high stress gradients are present, e.g. tests on pre-notched specimens. On the other hand, relevant scale effects are encountered also in uniaxial tensile tests on dog-bone shaped specimens [2, 3], where smaller stress gradients are present. In the latter case, size effects can not be predicted by the cohesive crack model.

In order to overcome the original cohesive crack model drawbacks, a *scale-independent* (or *fractal*) *cohesive crack model* has been proposed recently [4]. This model is based on the assumption of a fractal-like damage localization. The fractal nature of the damage process allows a consistent explanation of the size effects on the cohesive crack model parameters. As a matter of fact, if the damage zone is fractal both the geometrical quantities (i.e. the area of the resistant cross-section, the area of the final crack surface and the thickness of the damage band) and the physical quantities (i.e. the tensile strength, the fracture energy and the critical displacement) become nominal quantities and are, therefore, size-dependent. On the other hand, fractal quantities should be used: they are the true scale-invariant material parameters. The fractal strength and fractal fracture energy were introduced by Carpinteri in 1994 [5], while the fractal critical strain has been introduced recently [4, 6].

The hypothesis of a fractal damage domain received different experimental confirmations [7, 8]. The aim of the present paper is to provide a theoretical explanation of the fractality of the concrete damage domains based on the aggregate size distribution. As is well-known, the weakest link in normal strength concrete is represented by the interface between the cementitious matrix and the aggregates. Therefore it seems reasonable to look for a link between the aggregate grading and the fractal features (e.g. the fractal dimension) of the damage domain. Attention will be focused onto the computation of the fractal dimensions of (i) the region where energy is dissipated during the failure process and (ii) the region where stress is transferred at the peak load.

The main tool we will use to perform the fractal analysis is *Stereology*, which encompasses the geometrical probability aspects of the problem. For what concerns the stereology applied to concrete, we refer to the work by Stroeven [9–11], while useful fractal concepts can be found in the book by Turcotte [12], whose fragmentation analysis is analogous to the stereological approach we are going to develop.

It is found that the surface of the aggregates inside the damage band where the main crack will grow in the last stage of the tensile failure can be modelled by an invasive fractal set of dimension larger than 2. Furthermore, we obtain the probability density function of the diameters of the circles interception of the grains with a plane parallel to the damage band; this function shows that the resistant cross-section can be modelled by a lacunar fractal set with dimension lower than 2. Therefore lacunar and invasive fractalities are proven and consequent size effects on tensile strength and fracture energy may be pointed out.

2 The aggregate sieve curve and the related grain size distribution function

The basis for the dimensional characterization of the concrete aggregates is the sieve analysis. The sieve curve describes the weight percentage $W(d)$ of the aggregates passing through a sieve with d-wide mesh. Thanks to its good packing property, the most common sieve curve used to prepare concrete is the so-called Füller curve: $W(d) = \sqrt{d/d_{max}}$. Henceforth we will refer in the following to the Füller aggregate size distribution. Furthermore, we will assume the aggregates to be spheres of diameter d comprised between a maximum value, $d_{max} = 20$ mm, and a minimum one, $d_{min} = 0.2$ mm (hence $d_{min}/d_{max} = 1/100$). In large buildings, the largest size is usually proportional to the size of the structure: in dams, for instance, d_{max} can be set equal to 120 mm.

It can be easily shown [10] that the Füller sieve curve can be expressed in terms of grain size distribution function as follows:

$$f(d) = 2.5 \frac{d_{min}^{2.5}}{d^{3.5}} \tag{1}$$

where $f(d)$ is a probability density function (PDF), i.e. $f(d)\ \mathrm{d}d$ is the fraction of grains with diameter belonging to the interval $[d, d + \mathrm{d}d]$ and $\int_{d_{\min}}^{d_{\max}} f(d)\ \mathrm{d}d = 1$. Eq. (1) shows clearly that the number of the small particles is higher than that of the large ones, since the former must fill the gaps between the latter. We will mark by $\overline{d_{\mathrm{V}}}$, $\overline{d_{\mathrm{V}}^2}$, $\overline{d_{\mathrm{V}}^3}$ the first three moments of the PDF (1). The first moment represents the average diameter in the concrete volume, while the second and third are proportional to the average grain surface and volume, respectively.

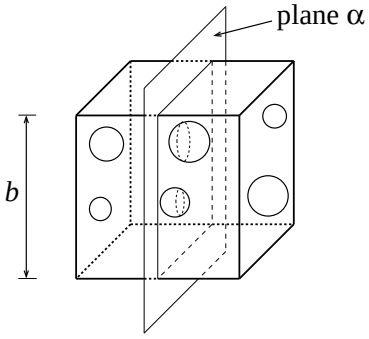

Figure 1: A concrete specimen: grain distribution in the bulk and on a plane α.

In order to study the weakening effect of the aggregates in the stress transfer mechanism inside concrete, the size distribution of the particles on a cutting plane is requested. To fix the ideas, let us refer to a concrete cube of side b cut by a plane α as shown in Fig. 1, where, for the sake of clarity, only a few particles have been drawn. We denote by N_{V} and N_{P} respectively the number of grains inside the volume and the number of grains intercepted by the plane α. Denoting by $g(d)$ the PDF of the grain diameters intercepted by the plane α, it is possible to prove

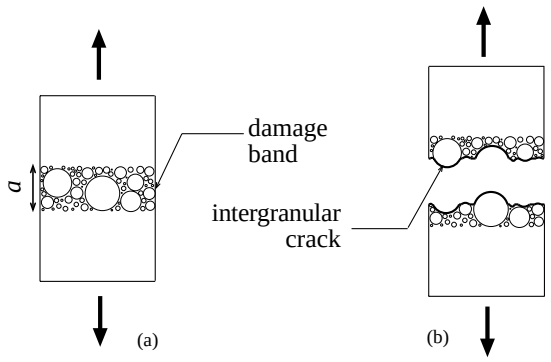

Figure 2: Concrete specimen tensile test: intergranular crack (a) and damage band (b).

the following relationships:

$$N_{\mathrm{P}} = \int_{d_{min}}^{d_{max}} \frac{d}{b} N_{\mathrm{V}}\ f(d)\ \mathrm{d}d = \frac{N_{\mathrm{V}}}{b}\ \overline{d_{\mathrm{V}}} \tag{2}$$

$$g(d) = \frac{d}{\overline{d_{\mathrm{V}}}}\ f(d) \tag{3}$$

Interestingly, the first moment of Eq. 3 (i.e. the average diameter $\overline{d_{\mathrm{P}}}$ of the particles intercepting the plane α) is higher than the average diameter in the bulk $\overline{d_{\mathrm{V}}}$. In the literature this phenomenon is called *coarsening*.

Eventually, wishing to find the relationship between the concrete volume and the number of grains inside it, we need one more parameter, i.e. the volume percentage f_a of the aggregates. This percentage must be rather high, since the aim is a good particle packing but also a sufficient fluidity of the mixture when the concrete is cast. In normal strength concrete the aggregates occupy about three fourth of the total volume; i. e. $f_a \simeq 0.75$. The total number of particles inside the cube of side b is, therefore:

$$N_{\mathrm{V}} = \frac{f_a b^3}{\frac{\pi}{6}\overline{d_{\mathrm{V}}^3}} \tag{4}$$

This means that, when the above data are considered, the particles inside $1\ \mathrm{m}^3$ of concrete are about 4 billions!

3 Fractal analysis of the aggregate-matrix interface

As will be shown in Section 5, according to the *fractal approach*, the size effect on the fracture energy can be explained only if the domain where energy is dissipated is fractal. If it is not, no size effect should be expected.

We will make two diffent hypotheses about the region where dissipation takes place and we will perform a fratal analysis of this region. With fractal analysis we mean essentially the computation of the fractal dimension of a given set. The easiest way to do it is possibly to measure the area of the set at different resolution levels and to study how the measure varies increasing the resolution. If it diverges, the set is an *invasive* fractal (i.e. with a dimension larger than 2); if it tends to zero, it is a *lacunar* fractal (i.e. with a dimension lower than 2); if it converges to a finite value different from zero, it is simply an Euclidean surface. The exponent of the power law describing the graph of the measure versus the resolution represents the difference from 2 of the fractal dimension of the given set. For the sake of simplicity, the resolution level will be identified by the grain diameter itself, even if, formally, the resolution should be the inverse of the diameter. For instance, a resolution of level d means to be able to capture the contribution of particles whose diameter is larger than or equal to d.

Now, let us consider the simple scheme of a uniaxial tensile test of the normal strength concrete specimen drawn in Fig. 2. As experimentally detected, we assume the crack to be intergranular (Fig. 2b); i.e. no grain breaks. The grains remain bonded to the side of the specimen containing their larger side. We further assume the portion of the crack that lies in the cementitious matrix to be flat.

About the energy dissipation region, we will make two different hypotheses: the former assumes this region to be the *crack surface* (Fig. 2b), the latter assumes as dissipation zone the surface of all the grains included in a *damage band* of thickness a (Fig. 2a).

For what concerns the former hypothesis, we see from Fig. 2b that the crack surface is composed by the surface of the cementitious matrix plus the surface of the grains. The area occupied by the matrix is simply equal to the fraction $1-f_a$ of the cross-section, while, increasing the measure resolution, more and more grains can be detected: hence the measure of the crack surface increases with the resolution. An upper bound for the portion of the crack area occupied by the grains is the sum S of the areas of the surfaces of all the grains cut by the plane of the crack, whose distribution is given by Eq. (3). S is a function of the resolution d according to:

$$S(d) = \int_d^{d_{max}} N_{\mathrm{P}}\, g(d)\, \pi d^2 \ \mathrm{d}d = \frac{5\pi N_{\mathrm{P}} d_{min}^{2.5} d_{max}^{0.5}}{\overline{d_{\mathrm{V}}}} \left(1 - \sqrt{\frac{d}{d_{max}}}\right) \tag{5}$$

As d tends to zero (infinite resolution), $S(d)$ converges to a finite value (see Fig.3). As stated above, this means that the crack surface is not a fractal set: it is simply a rough surface. Therefore, no size effect over the fracture energy should appear. Since this is not the case, we reject the former hypothesis and consider the latter one, according to which energy is dissipated over the interface between the matrix and the grains included in a a-wide damage band (Fig. 2a). In this case the area $A_{dis}(d)$ of all the interfaces is:

$$A_{dis}(d) = \int_d^{d_{max}} \frac{a}{b} N_{\mathrm{V}}\, \pi d^2 f(d) \ \mathrm{d}d = 5\pi \frac{a}{b} N_{\mathrm{V}} d_{min}^2 \left[\sqrt{\frac{d_{min}}{d}} - \sqrt{\frac{d_{min}}{d_{max}}}\right] \tag{6}$$

As the resolution increases (d tends to zero), $A_{dis}(d)$ diverges. This means that, in a certain range of scales, the set represented by the interfaces shows a fractal behaviour. Further, as shown in Fig. 3 where S and A_{dis} vs. measure resolution are plotted in a bilogarithmic, dimensionless diagram (assuming a equal to $3d_{max}$), Eq. (6) is very well approximated, for not too low resolutions, according to a power law with the exponent equal to -0.5: this fact allows us to state that the aggregate surface inside the damage band can be modeled by an *invasive fractal set* of dimension 2.5. The model is therefore able to predict the size effect on fracture energy in tensile tests, as will be pointed out in Section 5.

Finally, let us consider that, even if less intuitive in comparison with the former hypothesis about energy dissipation, there are experiments that lead to believe the latter hypothesis to be more realistic than the former one. For instance, acoustic emission analyses during tensile test performed by Shah over concrete specimens [13] showed that several damage phenomena take place inside the bulk all along the failure process. While at an early stage of loading they are spread all over the volume, near and after the peak load damage phenomena concentrate in a narrow band where, at the ultimate stage of the softening regime, the main crack appears. For these reasons, Bazant and Oh [14] developed their crack band model. Our model is however more complex, since we consider the damage to be fractal-like inside the damage band.

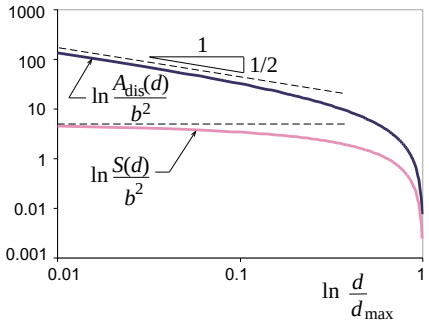

Figure 3: Bilogarithmic and dimensionless plot of the area S of the grains belonging to the fracture surface (gray line) and of the area A_{dis} of the aggregate-matrix interface inside the damage band (black line) vs. measure resolution.

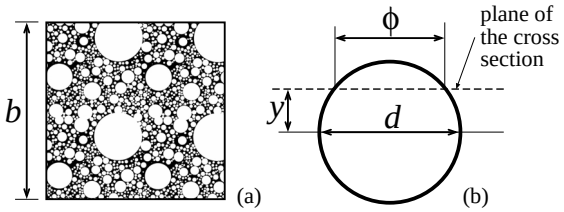

Figure 4: Cross-section of a concrete specimen: 2D distribution of the grain circles intercepted by the section plane (a) and detail of a particle (b).

4 Fractal analysis of the cementitious matrix cross-section

Now we turn our attention to the stress transfer inside the damage band of the concrete specimen subjected to a tensile load (Fig. 2a). As stated in the previous section, we assume that inside the damage zone, microcracks develop all around the aggregate near by the peak load. Therefore, the size distribution of the two-dimensional circles interception of the grains with the plane of the section (Fig. 4a) could be considered as representing the spatial size distribution of the initial bond cracks that have weakened the cross-section in an early stage of loading [9].

Denoting by ϕ the diameter of the circle intercepted by the section plane cutting a grain of diameter d (see Fig. 4b), the following relation holds:

$$y = \frac{\sqrt{d^2 - \phi^2}}{2} \tag{7}$$

where y is the distance of the center of the spherical grain to the plane of the cross-section. Based on the PDF $g(d)$ of the diameters d of the particles intercepted by a plane – see Eq. (3) – we intend to obtain the PDF $r(\phi)$ of the diameters ϕ of the circles belonging to the cross-section. The total number of circles belonging to the section is obviously N_{P} (Eq. (2)). The number of circles with diameter comprised between ϕ and $\phi + \mathrm{d}\phi$ is given by the sum of the compound events to find a particle with diameter $d \geq \phi$ whose center shows a distance from the section plane comprised between y and $y + \mathrm{d}y$. Since we deal with continuous distributions, the sum, in mathematical terms, is an integral between ϕ and d_{max}, if $\phi \geq d_{min}$, and between d_{min} and d_{max}, if $\phi < d_{min}$. On the other hand, the probability that the center of a sphere lies at a distance y from the section plane is $2\mathrm{d}y/d$ ($0 \leq y \leq d/2$). Therefore the number of circles with diameter comprised between ϕ and $\phi + \mathrm{d}\phi$ is:

$$N_{\mathrm{P}}\, r(\phi)\mathrm{d}\phi = \int_{d_{min},\phi}^{d_{max}} N_{\mathrm{P}}\, g(d)\, \frac{2\mathrm{d}y}{d}\mathrm{d}d \tag{8}$$

The link between y and ϕ is given by Eq. (7). Eq. (3) as well as the differentiation of Eq. (7) lead to the following result for the PDF $r(\phi)$:

$$r(\phi) = \begin{cases} \dfrac{\phi}{d_{\mathrm{V}}} \displaystyle\int_{d_{min}}^{d_{max}} \frac{f(d)}{\sqrt{d^2 - \phi^2}}\ \mathrm{d}d, & \text{if } 0 \leq \phi < d_{min} \\ \dfrac{\phi}{d_{\mathrm{V}}} \displaystyle\int_{\phi}^{d_{max}} \frac{f(d)}{\sqrt{d^2 - \phi^2}}\ \mathrm{d}d, & \text{if } d_{min} \leq \phi \leq d_{max} \end{cases} \tag{9}$$

In the case of the Füller sieve curve, $f(d)$ is given by Eq. (1) and no analytical solutions can be found for the function $r(\phi)$. However, an accurate numerical integration can be performed by means of the Gauss-Chebyshev quadrature formula. The result is plotted in Fig. 5a. Note that function $r(\phi)$ is continuous over the whole domain of existence, even if it has a singularity for $\phi = d_{min}$.

We are now able to compute the area A_{res} occupied by the cementitious matrix on a generic cross-section varying the measure resolution. As stated above, this area represents the true resistant cross-section at the peak load, since the bond cracks fully develop around the grains inside the damage band.

The area of the matrix (the black side of Fig. 4a) can be found by subtracting from the nominal area b^2 of the cross-section the area occupied by the grains. Increasing the measure resolution (i.e. decreasing ϕ), more and more grains can be detected and subtracted from the nominal area. That is:

$$A_{res}(\phi) = b^2 - \int_{\phi}^{d_{max}} N_{\mathrm{P}} r(\phi) \frac{\pi \phi^2}{4} \ \mathrm{d}\phi \tag{10}$$

Upon substitution of Eqs. (2) and (4) and dividing by b^2, we get:

$$\frac{A_{res}(\phi)}{b^2} = 1 - \frac{3 f_a \overline{d_{\mathrm{V}}}}{2 \overline{d_{\mathrm{V}}^3}} \int_{\phi}^{d_{max}} r(\phi) \phi^2 \ \mathrm{d}\phi \tag{11}$$

Using a numerical evaluation of $r(\phi)$, the dimensionless matrix area (11) can be plotted in Fig. 5b. In the same figure we plotted also the graph of the area of a deterministic fractal set of dimension 1.67, which is exactly a power law. The two curves are very close. We can therefore conclude that the resistant cross-section inside the damage band can be realistically modeled by a *lacunar fractal set* of dimension 1.67. Hence the model is able to predict the size effect on the tensile strength, as will be pointed out in Section 5.

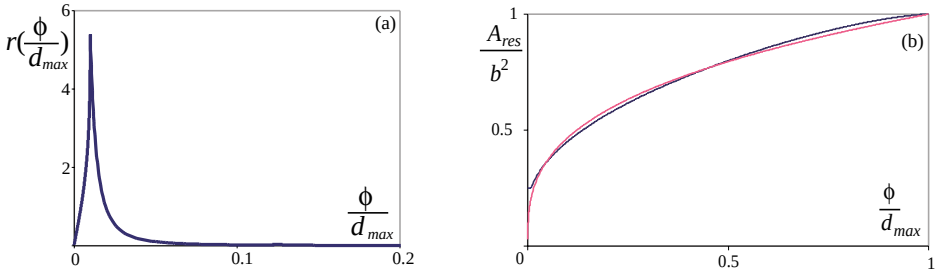

Figure 5: Probability density function of the diameters of the grain circles intercepted by the plane of the cross-section (a). Dimensionless area of the resistant cross-section (black line) and of a deterministic lacunar fractal set (gray line) vs. measure resolution (b).

Finally, let us consider that the fractal dimension of the resistant cross-section given by the analysis of Eq. (11) depends on the volume fraction occupied by the aggregates, f_a. More in detail, for very high values of the volume fraction ($f_a \simeq 0.9$) the fractal dimension tends to the value 1.5, while for low values of f_a it tends to 2, i.e. the dimension of an Euclidean surface. In other words, the aggregate are the cause of disorder inside the concrete microstructure. Eliminating the aggregates, both the fractal features and the related power laws describing the size effects of mechanical properties disappear (see next section).

5 Size-independent cohesive crack model

In the present section, the geometrical results of the fractal analysis of damage domains performed in the previous sections will be exploited to explain the size effects upon the mechanical quantities characterizing the cohesive law observed during experiments [2, 3, 5]. Besides, a fractal cohesive model independent of the structural size will be proposed.

First of all, let us consider the work W necessary to break a concrete specimen (Fig. 2) of cross section b^2. It is equal to the product of the fracture energy $\mathcal{G}_F$ times the nominal fracture area $A_0 = b^2$. On the other hand, we assumed that the surface where energy is dissipated is not the flat cross-section: it is the surface of the aggregates inside the damage band (Fig. 6c), whose area A_{dis} diverges as the measure resolution tends to infinity – see Eq. (6). Therefore the fracture energy should be zero, which is meaningless. Finite values of the measure of the set where energy is dissipated can be achieved only via the fractal (Hausdorff) measure [15] of the considered set, $A^*_{dis} \sim b^{2.5}$, to which the *fractal fracture energy* $\mathcal{G}^*_F$ corresponds [5]:

$$\begin{aligned} W = \mathcal{G}_F A_0 &= \mathcal{G}^*_F A^*_{dis} \\ \mathcal{G}_F &\sim \mathcal{G}^*_F b^{0.5} \end{aligned} \tag{12}$$

$\mathcal{G}_F^*$ is the true scale invariant material parameter, whereas the nominal value $\mathcal{G}_F$ is subjected to a scale effect described by a positive power law.

A similar argument holds for the tensile strength. The maximum tensile load F is equal to the product of the strength σ_u times the nominal area $A_0 = b^2$. On the other hand, we showed that the surface of the resistant cross-section is not the whole section: it is the portion of the surface occupied by the cementitious matrix (Fig. 6a), whose area A_{res} tends to zero as the measure resolution tends to infinite – see Eq. (11). Therefore, the strength should be infinite, which is meaningless. Finite values of the measure of the set where stress is transferred can be achieved only via the fractal (Hausdorff) measure [15] of the considered set, $A_{res}^* \sim b^{1.5}$, to which the *fractal strength* σ_u^* corresponds [5]:

$$\begin{aligned} F = \sigma_u A_0 &= \sigma_u^* A_{res}^* \\ \sigma_u &\sim \sigma_u^* b^{-0.5} \end{aligned} \tag{13}$$

σ_u^* is the true scale invariant material parameter, whereas the nominal value σ_u is subjected to a scale effect described by a negative power law. The absolute value 0.5 for the exponents of the power laws (12) and (13) is an upper bound, since they were derived according to the hypothesis that all the bond interfaces fail inside the damage band. More generally, therefore, the two power laws should be re-written as:

$$\mathcal{G}_F \sim \mathcal{G}_F^* b^{+d_\mathcal{G}} \tag{14}$$

$$\sigma_u \sim \sigma_u^* b^{-d_\sigma} \tag{15}$$

where $(2 + d_\mathcal{G})$ and $(2 - d_\sigma)$ are respectively the invasive and lacunar fractal dimensions of the domains where energy is dissipated and stress is tranferred. The two scaling exponents $d_\mathcal{G}$ and d_σ depend on the material and the kind of test. On the other hand, as we have shown, they are always positive and comprised between 0 and $1/2$. Finally, notice that the fractal fracture energy $\mathcal{G}_F^*$ and the fractal tensile strength σ_u^* show anomalous physical dimensions: respectively $[FL][L]^{-(2+d_\mathcal{G})}$ and $[F][L]^{-(2-d_\sigma)}$.

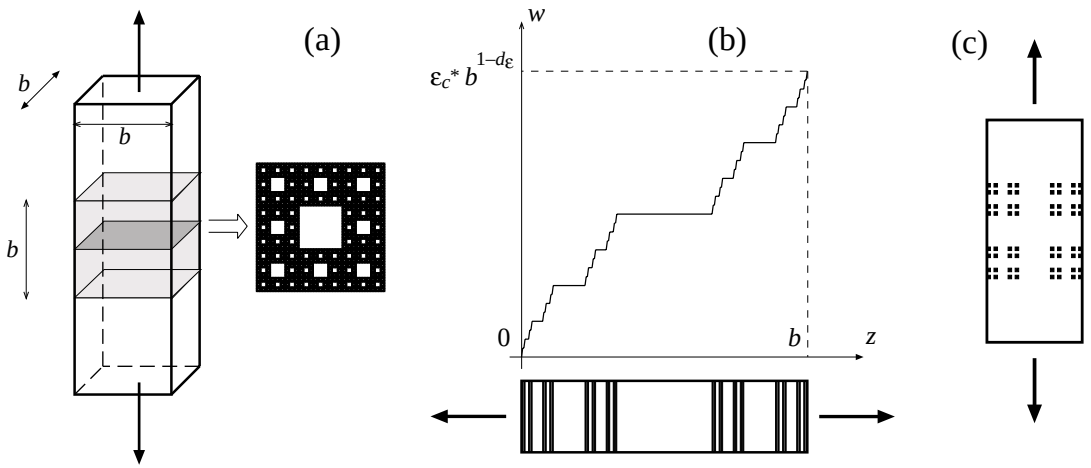

Figure 6: Fractal localization of stress (a), strain (b), energy dissipation (c).

Now we turn our attention to the deformation inside the damage zone. We assume that the strain field presents fractal patterns. This could appear strange at a first glance; on the contrary, fractal strain distributions are rather common in material science. For instance, in some metals, the so-called slip-lines develop with typical fractal patterns. Also fractal crack networks develop in dry clay or in old paintings under tensile stresses due to shrinkage. Thus, as representative of the damaged band, consider now the simplest structure, a bar subjected to tension (Fig. 6b), where, at the maximum load, dilation strain tends to concentrate into different softening regions, while the rest of the body undergoes elastic unloading.

Assume, for instance, that the strain is localized at cross-sections whose projections onto the longitudinal axis are provided by the triadic Cantor set, whose dimension is $\ln 2 / \ln 3 = 0.6391$; the displacement function at rupture

can be represented by a Cantor staircase graph, sometimes also called devil's staircase (Fig. 6b). The strain defined in the classical manner is meaningless in the singular points, as it diverges. This drawback can be overcome by introducing a fractal strain. Let us indicate with $1-d_\varepsilon$ ($d_\varepsilon \geq 0$) the fractal dimension of the lacunar projection of the damaged sections (in this case 0.6391). According to the fractal measure of the damage line projection, the total elongation w_c of the band at rupture must be given by the product of the Hausdorff measure $b^* \sim b^{(1-d_\varepsilon)}$ of the Cantor set times the *critical fractal strain* ε_c^*, while in the classical continuum theory it equals the product of the length b times the critical strain ε_c:

$$\begin{aligned} w_c = \varepsilon_c b &\sim \varepsilon_c^* b^{(1-d_\varepsilon)} \\ \varepsilon_c &\sim \varepsilon_c^* b^{-d_\varepsilon} \end{aligned} \tag{16}$$

where ε_c^* has the anomalous physical dimension $[L]^{d_\varepsilon}$. The fractal critical strain is the true material constant, i.e. it is the only scale-invariant parameter governing the kinematics of the fractal band. On the other hand, Eq. (16) states that the scaling of the critical displacement is described by a power law with positive exponent $(1-d_\varepsilon)$. The fractional exponent d_ε is intimately related to the degree of disorder in the mesoscopic damage process. When d_ε varies from 0 to 1, the kinematical control parameter ε_c^* moves from the canonical critical strain ε_c – of dimension $[L]^0$ – to the critical crack opening displacement w_c – of dimension $[L]^1$. Therefore, when $d_\varepsilon = 0$ (diffused damage, ductile behaviour), one obtains the classical response, i.e. collapse governed by the strain ε_c, independently of the bar length. In this case, continuum damage mechanics holds, and the critical displacement w_c is subjected to the maximum size effect ($w_c \sim b$). On the other hand, when $d_\varepsilon = 1$ (localization of damage onto isolated sections, brittle behaviour) fracture mechanics holds and the collapse is governed by the critical opening displacement w_c, which is size-independent as in the cohesive model.

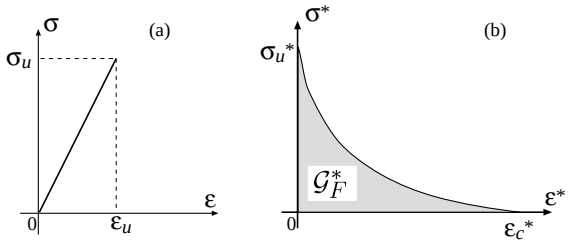

Figure 7: Fractal cohesive model.

The three size effect laws (14), (15), (16) of the cohesive law parameters are not completely independent one of the other. In fact, there is a relation among the scaling exponents that must be always satisfied. This means that, when two exponents are given, the third follows from the first two. In order to get this relation, suppose, for instance, to know d_σ and d_ε. Generalizing Eqs. (15) and (16) to the whole softening regime, we get $\sigma \sim \sigma^* b^{-d_\sigma}$ and $w \sim \varepsilon^* b^{(1-d_\varepsilon)}$. These relationships can be considered as changes of variables and applied to the integral definition of the fracture energy:

$$\mathcal{G}_F = \int_0^{w_c} \sigma \,\mathrm{d}w \sim b^{1-d_\varepsilon-d_\sigma} \int_0^{\varepsilon_c^*} \sigma^* \,\mathrm{d}\varepsilon^* = \mathcal{G}_F^* b^{1-d_\varepsilon-d_\sigma} \tag{17}$$

Eq. (17) highlights the effect of the structural size on the fracture energy, as Eq. (14) does. Therefore, comparing Eqs. (14) and (17), we get the relation among the exponents:

$$d_\sigma + d_\varepsilon + d_\mathcal{G} = 1 \tag{18}$$

Note that, from a physical point of view, the geometrical relationship (18) states that, after the peak load, the energy is dissipated over the infinite lacunar sections where softening takes place inside the damage band (Fig. 6a,b,c). While d_ε can get all the values inside the interval $[0,1]$, d_σ and $d_\mathcal{G}$ tend to be comprised between 0 and 1/2 (brownian disorder). Eq. (18) provides a strict restriction to the maximum degree of disorder, confirming that

the sum of d_σ and $d_\mathcal{G}$ is always lower than 1, as previously asserted by Carpinteri through dimensional analysis arguments [16].

It is interesting to note how, from Eq. (17), the fractal fracture energy $\mathcal{G}_F^*$ can be obtained as the area below the fractal softening stress-strain diagram (Fig. 7b). During the softening regime, i.e. when dissipation occurs, σ^* decreases from the maximum value σ_u^* to 0, while ε^* grows from 0 to ε_c^*. In the meantime, the nondamaged parts of the bar undergo elastic unloading (Fig. 7a). We call the σ^*- ε^* diagram the scale-independent or *fractal cohesive law*. Contrarily to the classical cohesive law, which is experimentally sensitive to the structural size, this curve should be an exclusive property of the material, it being able to capture the fractal nature of the damage process.

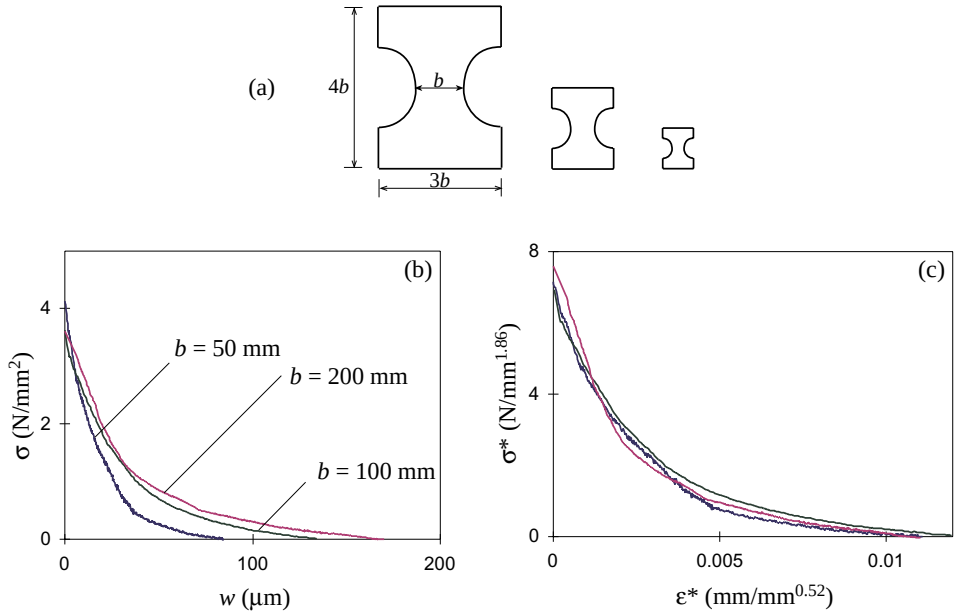

Figure 8: Tensile tests on dog-bone shaped concrete specimens (a) by Ferro [17]: cohesive law diagrams (b), fractal cohesive law diagrams (c).

The model has been applied to the data obtained in 1994 by Carpinteri and Ferro [2, 18] for tensile tests on dog-bone shaped concrete specimens of various sizes under controlled boundary conditions (Fig. 8a). They interpreted the size effects on the tensile strength and the fracture energy by fractal geometry. Fitting the experimental results, they found the values $d_\sigma = 0.14$ and $d_\mathcal{G} = 0.38$. Some of the σ-w diagrams are reported in Fig. 8b, where w is the displacement localized in the damage band, obtained by subtracting, from the total one, the displacement due to elastic and anelastic pre-peak deformation. Eq. (18) yields $d_\varepsilon = 0.48$, so that the fractal cohesive laws can be plotted in Fig. 8c. As expected, all the curves related to the single sizes tend to merge in a unique, scale-independent cohesive law. The overlapping of the cohesive laws for the different sizes proves the soundness of the fractal approach to the interpretation of concrete size effects.

More recently, van Mier and van Vliet [3] accurately performed tensile tests on dog-bone shaped concrete specimens over a wide scale range (1:32) under rotating boundary conditions (Fig. 10a). They plotted the cohesive law for specimens of different sizes and found that, increasing the specimen size, the peak of the curve decreases whereas the tail rises [20]. In other words σ_u decreases whereas w_c and $\mathcal{G}_F$ increases, thus confirming the prediction of the fractal model.

A preliminary analysis of the data obtained by van Mier and van Vliet [3] has been performed according to the fractal cohesive model. We considered the average values obtained for the different specimen sizes. The data of the smallest specimen size ($D = 50$ mm) were not considered, since, as stated by the authors, secondary effects are present (e.g. the influence of the largest grains and the wall effect) that bias the results. Furthermore, the authors were not able to obtain the whole tail of the softening branch for the specimens of the larger sizes. In order to obtain the value of the fracture energy, they completed the cohesive laws via a linear extrapolation. This

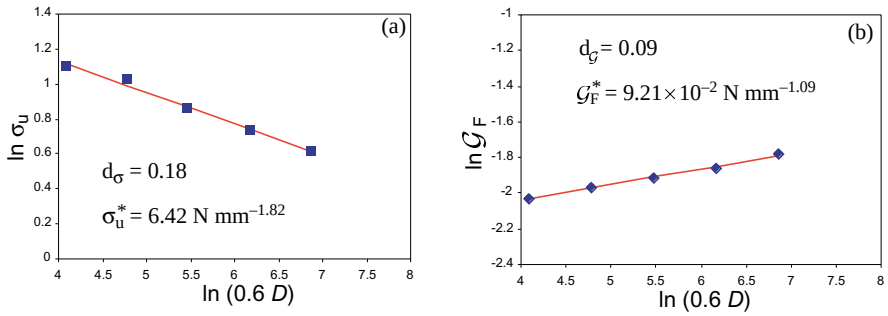

Figure 9: Tensile strength (a) and fracture energy (b) vs. specimen size: experimental data by Van Vliet [19] and linear interpolation in the bilogarithmic plot.

procedure, although rigorous, leads to an underestimate of the computed fracture energy since it does not respect the concavity of the curve. Therefore, we decided to complete the cohesive law diagrams in a somehow arbitrary way maintaining the concave shape for all the specimen sizes (Fig. 10b). Observing the interceptions of the curves with the axes, it is evident that the higher is the peak, the shorter is the tail.

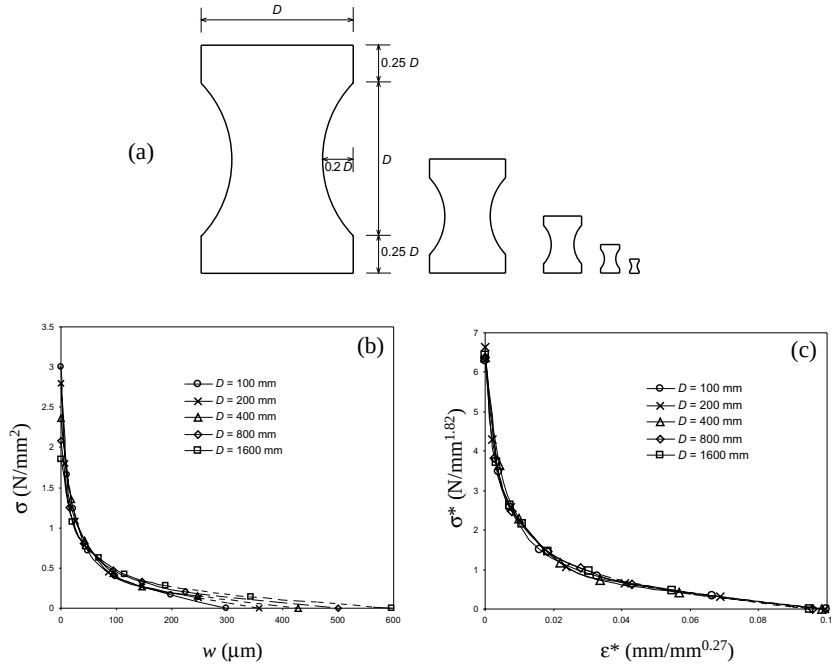

Figure 10: Tensile tests on dog-bone shaped concrete specimens (a) by van Vliet [19]: cohesive law diagrams (b), fractal cohesive law diagrams (c). The dashed lines refer to extrapolated values.

Linear regressions in the bilogarithmic plots of tensile strength and fracture energy vs. specimen cross section size were performed (Fig. 9). We found respectively a fractal fracture energy $\mathcal{G}_F^*$ equal to $9.22 \times 10^{-2} \mathrm{N\,mm}^{-1.09}$ and a fractal tensile strength σ_u^* equal to $6.42\ \mathrm{N\,mm}^{-1.82}$, with fractal exponents $d_{\mathcal{G}} = 0.09$ and $d_\sigma = 0.18$. The correlation coefficients were found to be respectively $R_{\mathcal{G}} = 0.995$ and $R_\sigma = 0.990$; their values close to unity prove the soundness of the power law scaling. The relation (18) among the scaling exponents yields $d_\varepsilon = 0.73$, so that the fractal cohesive laws can be plotted in Fig. 10c. Once again the superposition of the different plots denotes the validity of the fractal cohesive model. Particularly, note the low scattering of the interceptions with the vertical and horizontal axes in respect to the ones of Fig. 10b: they represent respectively the fractal critical strain ε_c^* and the fractal tensile strength σ_u^*, while the area subtended by the fractal cohesive law diagrams provides $\mathcal{G}_F^*$.

To conclude, it is worth observing how fractal patterns and related size effects, often detected in concrete tensile tests, can be seen as a consequence of the aggregate size distribution. Through stereological concepts and fractal analyses, we gave a theoretical description of the role of the aggregate in the tensile failure of concrete specimens. This seems particularly interesting, since, as pointed out recently [21], the aggregate is the cause of the tougher behavior of concrete with respect to mortar and hardened cement paste. Further experiments and analyses in this direction should be carried out in order to highlight the effects of aggregate grading and aggregate volume fraction.

6 Acknowledgements

Support by the MIUR and the EC-TMR Contract N° ERBFMRXCT 960062 is gratefully acknowledged by the authors.

References

[1] A. Hillerborg, M. Modéer, and P. E. Petersson. Analysis of crack formation and crack growth in concrete by means of fracture mechanics and finite elements. *Cement and Concrete Research*, 6:773–782, 1976.

[2] A. Carpinteri and G. Ferro. Size effects on tensile fracture properties: a unified explanation based on disorder and fractality of concrete microstructure. *Materials and Structures*, 28:563–571, 1994.

[3] J. G. M. Van Mier and M. R. A. Van Vliet. Effect of strain gradients on the size effect of concrete in uniaxial tension. *International Journal of Fracture*, 94:195–219, 1999.

[4] A. Carpinteri, B. Chiaia, and P. Cornetti. A scale-invariant cohesive crack model for quasi-brittle materials. *Engineering Fracture Mechanics*, 69:207–217, 2002.

[5] A. Carpinteri. Fractal nature of material microstructure and size effects on apparent mechanical properties. *Mechanics of Materials*, 18:89–101, 1994.

[6] A. Carpinteri and P. Cornetti. A fractional calculus approach to the description of stress and strain localization in fractal media. *Chaos, Solitons and Fractals*, 13:85–94, 2002.

[7] A. Carpinteri, B. Chiaia, and S. Invernizzi. Three-dimensional fractal analysis of concrete fracture at the meso-level. *Theoretical and Applied Fracture Mechanics*, 31:163–172, 1999.

[8] A. Carpinteri, B. Chiaia, and K.M. Nemati. Complex fracture energy dissipation in concrete under different loading conditions. *Mechanics of Materials*, 26:93–108, 1997.

[9] P. Stroeven. Structural modelling of plain and fibre reinforced concrete. *Composites*, pages 129–139, april 1982.

[10] P. Stroeven. Fractals and fractography in concrete technology. In A.M. Brand and I.H. Marshall, editors, *Brittle matrix composites 3*, pages 1–10. London: Elsevier Appl. Science, 1991.

[11] P. Stroeven. A stereological approach to roughness of fracture surfaces and tortuosity of transport paths in concrete. *Cement and Concrete Composites*, 22:331–341, 2000.

[12] D.L. Turcotte. *Fractal and Chaos in Geology and Geophysics*. Cambridge university press, 1997.

[13] S.P. Shah, S.E. Swartz, and C. Ouyang. *Fracture Mechanics of Concrete : Applications of Fracture Mechanics to Concrete, Rock and Other Quasi- Brittle Materials*. New York : John Wiley, 1995.

[14] Z.P. Bažant and B.H. Oh. Crack band theory for fracture of concrete. *Materials and Structures*, 16:155–177, 1983.

[15] J. Feder. *Fractals*. New York: Plenum Press, 1988.

[16] A. Carpinteri. Scaling laws and renormalization groups for strength and toughness of disordered materials. *International Journal of Solids and Structures*, 31:291–302, 1994.

[17] G. Ferro. *Effettti di Scala sulla Resistenza a Trazione dei Materiali*. PhD thesis, Politecnico di Torino, 1994.

[18] A. Carpinteri and G. Ferro. Scaling behaviour and dual renormalization of experimental tensile softening responses. *Materials and Structures*, 31:303–309, 1998.

[19] M. R. A. Van Vliet. *Size Effect in Tensile Fracture of Concrete and Rock*. PhD thesis, Technical University of Delft, 2000.

[20] J. G. M. Van Mier and M. R. A. Van Vliet. Experimental investigation of size effect in concrete under uniaxial tension. In H. Mihashi and K. Rokugo, editors, *Proceedings of "FRAMCOS-3"*, pages 1923–1936. AEDIFICATIO, 1998.

[21] B.L. Karihaloo and M.A. Tasdemir. Effect of type and volume fraction of aggregate on the fracture properties of concrete. In R. de Borst, J. Mazars, G. Pijaudier-Cabot, and J.G.M. Van Mier, editors, *Proceeding of FRAMCOS-IV*, pages 123–129. Balkema, 2001.